

Salicornia Begolovi as Eco-Friendly Corrosion Inhibitor for Aluminum in Hydrochloric Acid Solution

A. S. Fouda¹, S. M. Rashwan², A. E. Mohammed² and A. M. Ibrahim^{*2}

¹Department of Chemistry, Faculty of Science, Mansoura University, Mansoura-35516 and Department of Chemistry, Faculty of Science, Suez Canal University, Ismailia-41522, Egypt

THE INHIBITION effect of *Salicornia Begolovi* extract (SBE) as saving corrosion inhibitor for aluminum (Al) in 1 M HCl solution was studied using weight loss (WL), electrochemical impedance spectroscopy (EIS), electrochemical frequency modulation (EFM) and potentiodynamic polarization (PP) measurements. It was found that the *Salicornia* extract acts as a good inhibitor for aluminum corrosion in the acid solution. The inhibition efficiency (IE) increases with increasing of both extract dose and temperature, indicating that this extract was adsorbed chemically on Al surface. PP studies indicated that the extract acts as a mixed type inhibitor. EIS studies showed a reduction in the double layer capacitance and an increase in the charge transfer resistance. The adsorption of extract molecules was found to obey Temkin adsorption isotherm. The extract provides a good protection film to aluminum against corrosion in HCl solutions. Surface analysis was tested using scanning electron microscope (SEM). The results obtained from all investigated techniques are in good agreement.

Keywords : Acid inhibition, Aluminum, SBE, WL, EIS, EFM, SEM.

Introduction

Aluminum and its alloys represent an important category of materials due to their high technological value and wide range of industrial applications, especially in aerospace, automobile and household industries. Aluminum alloys enjoy a wide range of commercial usage due to their numerous desirable properties such as excellent mechanical properties, high strength, low density, lightweight, high thermal conductivity. However, they are reactive materials and are prone to corrosion [1]. Al-2Mg alloy is used for tank heating coils in crude-oil carriers. HCl is widely used in acid pickling, acid cleaning and oil well acidizing. Besides, acids increase rate of metal dissolution and are responsible for material failure indirectly. So, it is an important to use corrosion inhibitors to decrease metal dissolution. The most important problem in this area of research is related to the protection of Al and its alloys against corrosion. One of the most important methods against the corrosion is to use inhibitors. The most role of inhibitor is to prevent the metal from the corrosive medium or to modify the electrode reactions that cause dissolution of the metal. Most of the efficient acid inhibitors are

organic compounds that contain mainly nitrogen, sulphur or oxygen atoms in their structure [2-6]. The inhibition efficiency (IE) of organic compounds is strongly dependent on the structure and chemical properties of the layer formed on metals. Heterocyclic compounds are well known for their efficiencies as corrosion inhibitors and those containing nitrogen have been frequently referred to in the literature [7-9]. Because of the broad spectrum of organic compounds available as corrosion inhibitors, there is increasing concern about the toxicity of most corrosion inhibitors because they are toxic to living organism and may be poison the earth [10]. These have promoted searches for green corrosion inhibitors. According to Eddy et al. [11], green corrosion inhibitors are biodegradable and do not contain heavy metals or other toxic compounds.

The use of photochemical as natural antimicrobial agents, commonly called 'biocides' is gaining popularity. The most essential of these bioactive constituents of plants are alkaloids, tannins, flavonoids and phenolic compounds. Many of the indigenous medicinal plants are used as spices and food. Phytoconstituents have found

applications as naturally occurring antimicrobial agents in the field of preservation, pharmaceuticals, phytopathology, etc. Increasing failure of chemotherapeutics and the resistance exhibited by pathogenic microbial infectious agents against antibiotics have led to the screening of medicinal plants for their potential antimicrobial activities. There are several reports regarding the antimicrobial activity of crude extracts prepared from plants. Some of the active principles of the bioactive compounds are preferred to for their therapeutic purposes either as a single entity or in combination, so as to inhibit the life processes of microbes. Of recent times, most of the industries are made by the use of natural materials for preservation [12].

The present research will discuss the *Salicornia Begolovi* extract (SBE) as a green corrosion inhibitor which as renewable source, friendly environmental acceptance, biodegradable, safer and cheaper than other green corrosion inhibitors for protecting Al in 1 M HCl medium.

Experimental Methods

Materials and Solutions

The working electrode for weight loss (WL) and electrochemical studies were prepared from Al specimens (99.98%). The specimens were mechanically abraded with different grades of silicon carbide papers (320- 2000) then washed with a double distilled water, and dried at room temperature. The aggressive solution used was prepared by dilution of analytical reagent grade 37% HCl with double distilled water. The stock solution (1000 ppm) of SBE was used to prepare the desired doses by dilution with double distilled water. The concentration range of SBE used was 50-300 ppm.

Preparation of plant extracts

Fresh aerial parts of *Salicornia* Extracts sample were crushed to make fine powder. The powdered materials (250 g) were soaked in 500 ml of dichloromethane for 5 days and then subjected to repeated extraction with 5×50 ml until exhaustion of plant materials. The extracts obtained were then concentrated under reduced pressure using rotary evaporator at temperature below 50°C. The dichloromethane evaporated to give solid extract which was cooled and stored at room temperature and ready for use as corrosion inhibitor.

Weight loss (WL) technique

The specimens dimension for the weight loss (WL) test were 2 cm × 2 cm × 2 cm. Both sides of the specimens were exposed for WL test. After accurate weighing, the specimens were immersed in 250 ml beaker, which contained 100 ml of 1 M HCl with and without addition of different doses of SBE. All the aggressive acid solutions were open to air. The inhibition efficiency for weight loss (%IE_{wl}) was evaluated after a pre-optimized time interval of 3 hours using 50-300 ppm of the extract. After 3 hours, the specimens were removed from the electrolyte, washed thoroughly with double distilled water, dried and weighed. The average weight loss of seven parallel aluminum sheets could be obtained. The inhibition efficiency (%IE_{wl}) and the degree of surface coverage, θ of SBE for the corrosion of Al were calculated as follows [13]:

$$\%IE_{wt} = \left[1 - \frac{W^0}{W} \right] \times 100 = \theta \times 100 \quad (1)$$

where W^0 and W are the values of the average weight losses (mg) without and with addition of the extract, respectively.

Electrochemical technique

The electrochemical experiments were performed in a three-necked glass assembly containing 100 ml of the electrolyte with different doses of extract (50-300 ppm). All electrochemical tests were carried out with Al sheet working electrode having an exposed area of 1 cm². A conventional three-electrode cell consisting of Al as a working electrode, platinum foil as a counter electrode, and a saturated calomel electrode as a reference (SCE) electrode was used. All the measurements were done in solutions open to atmosphere under unstirred conditions. All potential values were reported versus SCE. Prior to each experiment, the electrode was abraded as before, washed with double distilled water, and finally dried. Tafel polarization curves were obtained by changing the electrode potential automatically from (-0.8 to 1 V vs. SCE) at open circuit potential with sweep rate of 1 mVs⁻¹. For calculating the inhibition efficiency (%IE_p) and surface coverage (θ) the following formula was used:

$$\%IE_p = \left[1 - \frac{i_{corr(inh)}}{i_{corr(free)}} \right] \times 100 = \theta \times 100 \quad (2)$$

where $i_{\text{corr(free)}}$ and $i_{\text{corr(inh)}}$ are the corrosion current densities in the absence and presence of inhibitor, respectively.

Alternating current (AC) impedance measurements were acquired the frequency range of 2×10^4 Hz to 8×10^2 Hz at rest potential by applying 10mV sine-wave AC voltage. The experimental impedance was analyzed and interpreted based on the equivalent circuit. The charge transfer resistance (R_{ct}) and the double layer capacitance (C_{dl}) were determined from Nyquist plots. The inhibition efficiency (%IE_{EIS}) and the surface coverage (θ) were calculated from R_{ct} values using the following formula:

$$\%IE_{\text{EIS}} = \left[1 - \left(\frac{R_{\text{ct}}}{R_{\text{ct}}^0} \right) \right] \times 100 = \theta \times 100 \quad (3)$$

where R_{ct}^0 and R_{ct} are the charge transfer resistance in the absence and presence of inhibitor, respectively.

Electrochemical frequency modulation, EFM, was carried out using two frequencies 2 and 5 Hz. The base frequency was 0.1 Hz, so the waveform repeats after 1 s. The large peaks were used to calculate the corrosion current density (i_{corr}), the Tafel slopes (β_a and β_c) and the causality factors CF-2&CF-3 [14].

All electrochemical tests were performed using Gamry Instrument (PCI4/750 Potentiostat/Galvanostat/ZRA). This includes a Gamry framework system based on the ESA 400. Gamry applications include DC105 software for polarization, EIS300 software for EIS and EFM140 software for EFM measurements via computer for collecting data. Echem Analyst 6.03 software was used for plotting, graphing, and fitting data. To test the reliability and reproducibility of the measurements, triplicate experiments were conducted at the same conditions. For all tests, the electrode potential was allowed to stabilize 30 min before starting the measurements. All the experiments were conducted at 25°C.

Surface analysis

For morphological study, surface features (2 cm x 2 cm x 2cm) of Al were examined before

and after exposure to 1 M HCl solutions for one day with and without inhibitor. JEOL JSM-5500 scanning electron microscope was used for this investigation.

Results and Discussion

Potentiodynamic polarization technique

Potentiodynamic polarization (PP) curves recorded for Al in 1 M HCl solutions in the absence and presence of various doses of SBE at 25°C as shown in Fig. 1. The polarization curves remain almost the same in the absence of the extract, but in the presence of extract both anodic and cathodic branches shifted to the lower values of corrosion current densities compared to the blank solution. The electrochemical parameters derived from the polarization curves in Fig. 1 are given in Table 1. It is noted from this Table that i_{corr} values decrease with the increase of the dose of extract, due to the increase in the blocked fraction of the Al surface by adsorption of extract components. The Tafel slopes of β_a and β_c at 25°C do not change remarkably upon addition of SBE, which indicates that both anodic and cathodic processes are controlled. A small shift in E_{corr} values towards positive direction was obtained in the presence of the extract indicating that the mixed nature of the extract. Generally, an inhibitor can be classified as cathodic or anodic type if the shift of corrosion potential in the presence of the inhibitor is more than 85 mV with respect to that in the absence of the inhibitor [15,16]. In our test, the maximum shift is about 20-30 mV, which indicates that SBE can be arranged as mixed-type inhibitor.

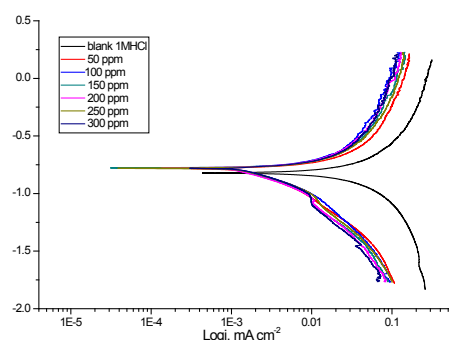


Fig.1. PP curves for the corrosion of Al in 1 M HCl solution without and with various doses of SBE at 25°C.

Electrochemical impedance spectroscopy (EIS) technique

Nyquist plots for Al in 1 M HCl solution

without and with various doses of SBE (50-300 ppm) are shown in Fig. 2. All Nyquist plots obtained were semicircle in nature, the diameter of the semicircles improved with improve in extract doses, and the shape remains constant through the test, indicating that the corrosion proceeds mainly under charge-transfer control and the presence of extract does not alter the mechanism of corrosion reaction. It is found that the obtained Nyquist plots are not perfect semicircle due to frequency dispersion and this behavior can be attributed to roughness and in-homogeneities of the electrode surface [17]. When there is non-ideal frequency response, it is common practice to use distributed circuit elements in an equivalent circuit. The most widely employed is the constant phase element (CPE). In general a CPE is used in a model in place of a capacitor to compensate for in-homogeneity in the system [18]. The electrical equivalent circuit model shown in Fig. 3 was used to analyze the obtained impedance data. The model consists of the solution resistance (R_s), the charge-transfer resistance of the interfacial corrosion reaction (R_{ct}) and the constant phase angle element (CPE). The value of frequency power (n) of CPE ($-1 \leq n \leq +1$), can be assumed

to correspond to capacitive behavior. However, excellent fit with this model was obtained with our experimental data. It was found that the diameters of the semicircle increases with increasing the dose of the investigated extract. This indicates that the polarization resistance of the oxide layer increases with increasing the dose of SBE and the depressed capacitive semicircle is often referred to the surface roughness and in-homogeneity, since this capacitive semicircle is correlated with dielectric properties and thickness of the barrier oxide film [19]. In addition, to the high frequency capacitive loop, the semi-circles rolled over and extended to the fourth quadrant, and a pseudo-inductive loop at low frequency end was observed, indicating that Faradic process is taking place on the free electrode sites. This inductive loop is generally attributed to the adsorption of species resulting from the Al dissolution and the adsorption of hydrogen [20]. The double layer capacitance (C_{dl}) for a circuit including a CPE was calculated from the following equation:

$$C_{dl} = Y_0 (\omega_{max})^{n-1} \quad (4)$$

where $\omega_{max} = 2\pi f_{max}$, f_{max} is the frequency at which

TABLE 1. Electrochemical parameters calculated using PP technique for the corrosion of Al in 1 M HCl in the absence and presence of SBE at 25°C.

[inh], ppm	i_{corr} , mA cm ⁻²	$-E_{corr}$, mV vs. SCE	β_a , mVdec ⁻¹	β_c , mVdec ⁻¹	C.R.X10 ⁻³ mpy	θ	%IE
1 M HCl	48.3	821	240	390	207	-----	----
50	4.24	777	206	428	18.2	0.912	91.2
100	3.1	780	138	486	13.2	0.935	93.5
150	2.86	779	142	436	12.3	0.941	94.1
200	2.72	779	150	407	11.6	0.944	94.4
250	2.1	784	110	394	9.0	0.957	95.7
300	1.77	775	120	394	7.6	0.964	96.4

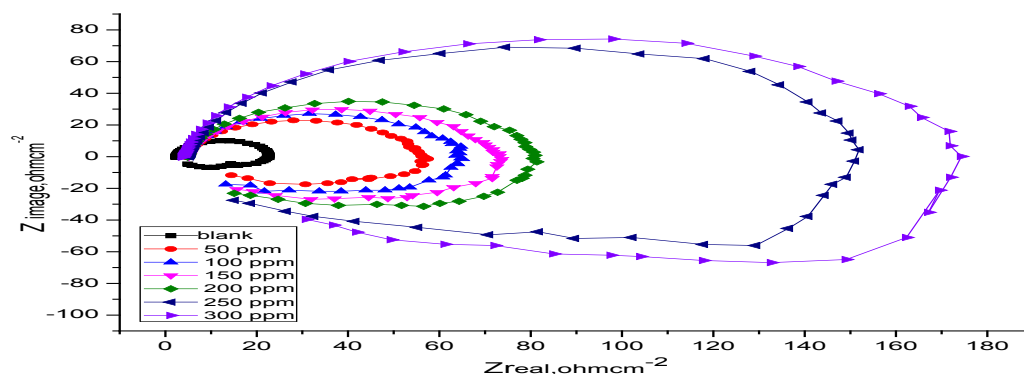


Fig. 2. Nyquist plots for Al in 1 M HCl solutions with and without various doses of SBE at 25°C.

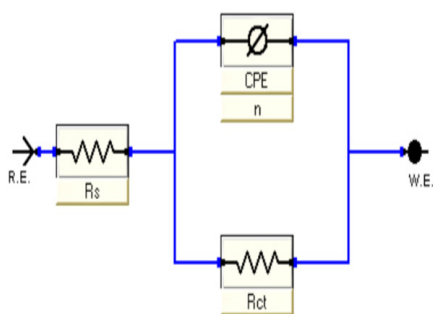


Fig. 3. Equivalent circuit used to model impedance data for Al in 1 M HCl solutions.

the imaginary component of the impedance is maximal and n is the CPE exponent (phase shift).

The electrochemical parameters calculated from Nyquist plots using the equivalent circuit (Fig.3) are presented in Table 2.

Since the electrochemical theory assumed that $(1/R_{ct})$ is directly proportional to the capacity of double layer C_{dl} , the %IE of the extract for Al in 1 M HCl solution was calculated from R_{ct} values obtained from impedance data at different inhibitor doses by using equation (3).

From the impedance data given in Table 2, we can conclude that the value of R_{ct} increases with the increase in the dose of the SBE and this indicates the formation of a protective film on the Al surface by the adsorption and an increase in the corrosion IE in acidic solution. While the value of C_{dl} decreases with increasing the doses of the extract in comparison with that of blank solution (uninhibited), as a result from the replacement of water molecules by inhibitor molecules which lead to decrease in local dielectric constant and/or an increase in the thickness of the electric double layer formed on the metal surface [21].

Electrochemical frequency modulation (EFM) technique

EFM is a nondestructive corrosion measurement technique that can directly determine the corrosion current value without prior knowledge of Tafel slopes, and with only a small polarizing signal. These advantages of EFM technique make it an ideal candidate for online corrosion monitoring [22]. The great strength of the EFM is the causality factors which serve as an internal check on the validity of EFM measurement. The EFM intermodulation spectrums of Al in 1 M HCl solution containing (50- 300ppm) of the SBE at 25°C are shown in

Fig.4. The larger peaks were used to calculate the corrosion current density (i_{corr}), the Tafel slopes (β_c and β_a) and the causality factors (CF-2 and CF-3) [23]. These electrochemical parameters are listed in Table 3 indicating that this extract inhibits the corrosion of Al in 1 M HCl through adsorption. The causality factors obtained under different experimental conditions are approximately equal to the theoretical values (2 and 3) indicating that the measured data are verified and of good quality [24]. The IE_{EFM} increases by increasing the studied extract doses and was calculated as follows:

$$\%IE_{EFM} = \left(\frac{i_{corr}^0 - i_{corr}}{i_{corr}} \right) \times 100 = \theta \times 100 \quad \dots\dots\dots(5)$$

where i_{corr}^0 and i_{corr} are corrosion current densities in the non-existence and existence of SBE, respectively.

Weightloss technique

WL-time curves were carried out for Al in 1 M HCl in the absence and presence of different doses of SBE at 25°C and are shown in Fig.5. The %IE values calculated are listed in Table 4. From this Table, it is noted that the corrosion rate decreases and the %IE increases as the doses of SBE increase at 25°C. The %IE and surface coverage (θ) were calculated by equation (1). The observed inhibition action of the SBE could be attributed to the adsorption of its components on Al surface. The formed layer of the adsorbed molecules isolates the metal surface from the aggressive medium which limits the dissolution of Al by blocking of their corrosion sites and hence decreasing the corrosion rate, with increasing efficiency [25].

Effect of temperature

WL method was carried out at different temperatures (25°C–45°C) in the presence of different doses of SBE. It has been found that the corrosion rate improves with improving in temperature for SBE (Table 5). The corrosion rate of Al in the absence of SBE increased steeply from 25 to 45°C whereas; in the presence of SBE the corrosion rate decreased slowly. The rate of corrosion increases with increase in temperature (Table 5) and hence, increases in %IE as shown in Fig. 6.

Kinetic and thermodynamic study

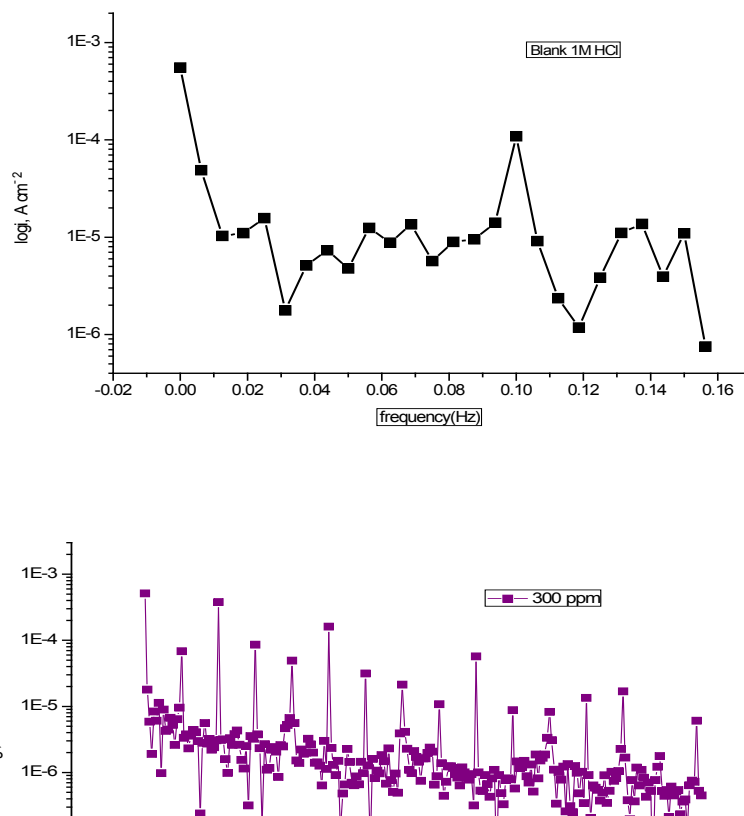
The corrosion parameter in the absence and presence of SBE in the temperature range 25–45°C has been summarized in Table 6. The

TABLE 2. Electrochemical parameters obtained from EIS technique for the corrosion of Al 1 M HCl solutions with and without the existence of various doses of SBE at 25°C.

Conc, ppm.	R_s , Ωcm^2	n	Y^0 , $\mu\Omega^{-1}\text{s}\text{cm}^{-2}$	R_{ct} , Ωcm^2	C_{dl} , $\mu\text{F}\text{cm}^{-2}$	θ	% IE
1 M HCl	2.4	0.872	32.0	11.8	7.9	-----	-----
50	4.5	0.854	23.4	36.2	7.6	0.674	67.4
100	4.4	1.03	5.0	36.5	6.7	0.677	67.7
150	5.3	1.02	4.7	40.6	5.3	0.71	71.0
200	5.2	1.0	4.3	43.1	4.4	0.727	72.7
250	5.4	1.01	4.2	49.5	3.8	0.762	76.2
300	3.9	1.0	2.8	77.1	3.0	0.847	84.7

TABLE 3. Electrochemical kinetic parameters obtained by EFM technique for Al in 1 M HCl solutions containing various doses of SBE at 25°C.

[inh], ppm	i_{corr} , $\mu\text{A}\text{cm}^{-2}$	β_a , mVdec^{-1}	β_c , mVdec^{-1}	C.R. $\times 10^{-3}$, mpy	CF-2	CF-3	θ	% IE
1 M HCl	378	46	231	1.62	1.96	1.9	-----	-----
50	294	39	143	1.26	1.8	1.7	0.223	22.3
100	240	34	44	1.02	2.3	2.5	0.365	36.5
150	192	29	58	0.825	2.3	2.1	0.50	50
200	181	30	41	0.782	2.7	2.0	0.521	52.1
250	169	29	48	0.726	2.2	2.1	0.553	55.3
300	136	27	41	0.582	1.8	2.0	0.641	64.1

**Fig. 4.** Intermodulation spectrums for the corrosion of Al in 1 M HCl without and with various doses of SBE at 25°C.

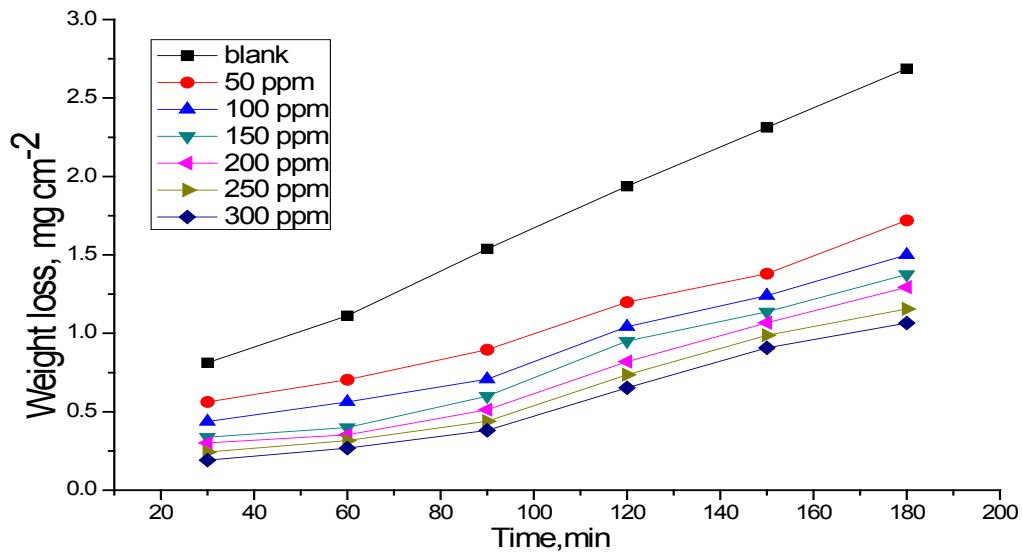


Fig. 5. WL-time curves for the corrosion of Al in 1 M HCl with and without existence of different doses of SBE at 25°C.

TABLE 4. WL measurements data for Al in 1 M HCl solution with different doses of SBE after 120 minutes of immersion at 25°C.

[Inh]. ppm	WL, mg cm ⁻²	$k_{\text{corr}} \times 10^3$ mg cm ⁻² min ⁻¹	θ	%IE
1M HCl	1.93	16.14	-----	-----
50	1.11	9.26	0.426	42.6
100	1.0	8.33	0.484	48.4
150	0.951	7.92	0.509	50.9
200	0.863	7.19	0.554	55.4
250	0.813	6.77	0.581	58.1
300	0.750	6.25	0.613	61.3

apparent activation energy (E_a^*) for dissolution of Al in 1M HCl was calculated from the slope of plots by using Arrhenius equation:

$$\log k = \frac{-E_a^*}{2.303 RT} + \log A \quad \text{.....(6)}$$

where k is rate of corrosion, E_a^* is the apparent activation energy, R is the universal gas constant, T is absolute temperature and A is the Arrhenius pre-exponential factor.

By plotting $\log k$ against $1/T$, the values of E_a^* have been calculated ($E_a^* = \text{slope} \times 2.303 \times R$) in Fig.

7. E_a^* values increase in the presence of SBE for Al in 1M HCl (Table 6). The decrease in E_a^* with increase inhibitor dose of extract is typical of chemisorption due to the chemical bonds were strengthened by increasing temperature of energy barrier on the Al surface and its thickness increases by increasing the doses. This indicative to the physical adsorption of extract molecules on the Al surface as reported before [26]. The values of change of entropy (ΔS^*) and change of enthalpy (ΔH^*) can be calculated by using the formula:

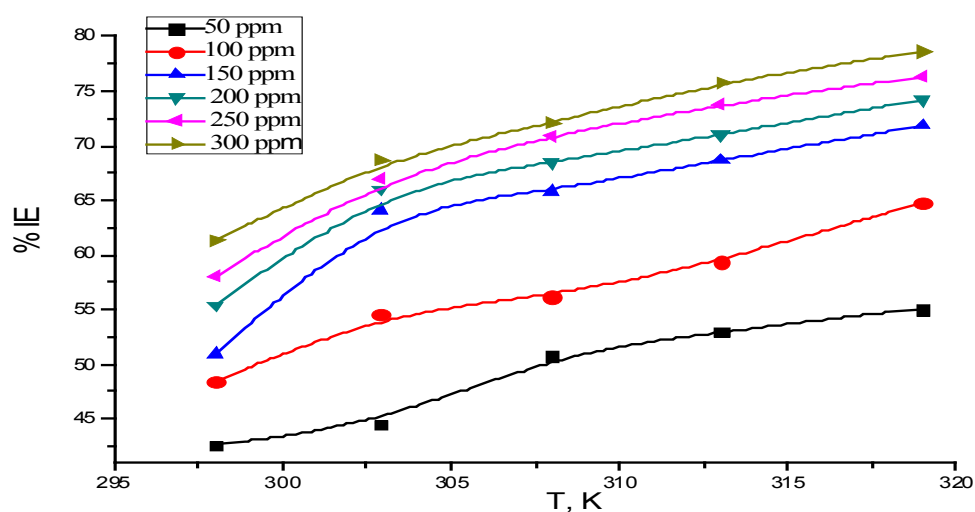


Fig. 6. Effect of temperature on %IE using various doses of SBE on Al surface in 1 M HCl at different temperatures.

TABLE 5. Data of WL measurements for Al in 1 M HCl solution with different doses of SBE after 120 min of immersion at 30 - 45°C.

%IE	θ	$k_{\text{corr}} \times 10^3$ $\text{mg cm}^{-2} \text{min}^{-1}$	WL, mg cm^{-2}	[Inh]. ppm	Temp., K
-----	-----	33.03	3.96	Blank	
43.2	0.432	18.96	2.27	50	303
55.5	0.555	14.58	1.75	100	
64.4	0.644	11.77	1.41	150	
65.3	0.653	11.45	1.37	200	
67.8	0.678	10.61	1.27	250	
68.4	0.684	10.02	2.16	300	
-----	-----	64.86	7.78	Blank	
51.9	0.519	31.11	3.73	50	308
55.8	0.558	27.34	3.28	100	
65.3	0.653	21.83	2.62	150	
68.5	0.685	20.41	2.45	200	
70.9	0.709	18.83	2.26	250	
72.1	0.721	13.85	4.62	300	
-----	-----	159.22	19.11	Blank	
52.2	0.522	75.92	9.11	50	313
59.4	0.594	64.56	7.74	100	
68.7	0.6389	49.82	5.98	150	
71	0.710	46.16	5.54	200	
73.8	0.738	41.71	5.00	250	
75.78	0.7578	38.42	4.62	300	
-----	-----	218.70	26.25	Blank	
54.7	0.547	99.23	11.90	50	318
61.9	0.619	83.68	10.06	100	
71.8	0.71.8	61.75	7.41	150	
74.2	0.742	56.49	6.77	200	
76.3	0.763	52.11	6.25	250	
78.6	0.786	46.86	5.62	300	

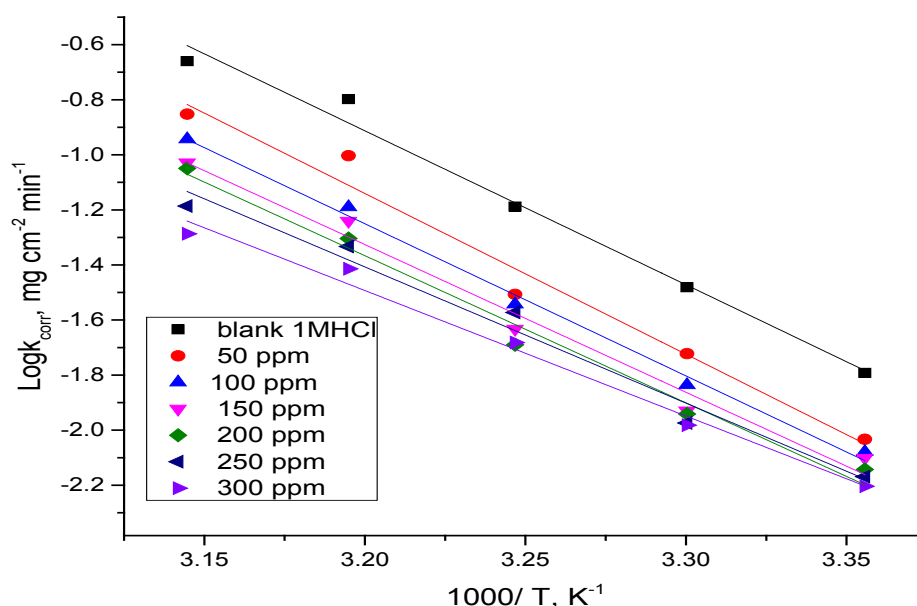


Fig. 7. Arrhenius plot (logk vs.1/T)for Alin 1 M HClwith and without presence of various concentrations ofSBE

$$k = \left(\frac{RT}{Nh}\right) \exp\left(\frac{\Delta S^*}{R}\right) \exp\left(\frac{\Delta H^*}{RT}\right) \quad (7)$$

where h is Planck's constant, N is Avogadro number.

A plot of $\log(k/T)$ vs. $1/T$ (Fig. 8) should give a straight line, with a slope of $(\Delta H^*/2.303R)$ and an intercept of $[\log(R/Nh) + \Delta S^*/2.303R]$, from which the values of ΔS^* and ΔH^* can be calculated (Table 6). The positive signs of the enthalpies (ΔH^*) reflect the endothermic nature of the Al dissolution process. decreasing in the values of ΔS^* for the extract imply that activated complex in the rate-determining step represents the dissociation rather than association step, indicating that an increase in disorder takes place on going from reactants to the activated complex [27]. The positive sign of ΔH^* revealed the endothermic nature of the corrosion process.

Generally, an endothermic process indicates chemisorption. various concentrations of SBE.

Adsorption isotherms

The adsorption isotherms were conducted to have more insight into the mechanism of corrosion inhibition. Because the IE of metals is usually due to either the adsorption of the inhibitor molecules on the metal surface or the formation of a film of insoluble metal complexes [28]. To obtain the adsorption isotherms, the degree of surface coverage obtained from WL method was determined as a function of dose extract. The values of θ were then plotted to fit the most suitable model of adsorption [29]. To determine the adsorption mode, Temkin adsorption isotherms as shown in Fig. 9 was found to be the best, which give a straight line graph for the plot of θ versus $\log C$ [30]. An adsorption isotherm gives the relation between the coverage of an interface with the adsorbed species and the dose of the species in solution. Interpretation of the performance of the adsorbent type of

TABLE 6. Activation parameters for dissolution of Al in the absence and presence of different doses of SBE in 1 M HCl

[inh], ppm	$-E_a^*$, kJ mol ⁻¹	ΔH^* , kJ mol ⁻¹	ΔS^* , J mol ⁻¹ K ⁻¹
1 M HCl	107	105	74
50	111	110	83
100	105	104	62
150	102	100	51
200	102	98	48
250	94	92	22
300	87	86	2

inhibitor can be enhanced by fitting the data in one of known adsorption isotherm which is represented in Fig. 9. Temkin adsorption isotherm [31] fits well the experimental data.

$$\theta_{\text{coverage}} = \left(\frac{2.303}{a}\right) \log K_{\text{ads}} + \left(\frac{2.303}{a}\right) \log C \quad \dots\dots\dots(8)$$

where K_{ads} is the adsorption equilibrium constant and “a” (heterogeneous factor of metal surface) is a molecular interaction parameter depending upon molecular interactions.

A plot of θ versus $\log C$ should give straight lines with slope equals $(2.303/a)$ and the intercept is $(2.303/a) \log K_{\text{ads}}$. The experimental data give good curves fitting for the applied adsorption isotherm as the correlation coefficients (R^2) close to unit. The values obtained of “a”, K_{ads} and $\Delta G_{\text{ads}}^\circ$ are given in Table 7. K_{ads} can be calculated from the intercept of fitting formula in Fig 9. The relationship of K_{ads} and standard free energy ($\Delta G_{\text{ads}}^\circ$) can be expressed by Eq.10.

$$\Delta G_{\text{ads}}^\circ = -RT \ln(55.5 K_{\text{ads}}) \quad \dots\dots\dots(9)$$

where 55.5 is the molar concentration of water in M^{-1} .

The negative value of $\Delta G_{\text{ads}}^\circ$ indicates spontaneous adsorption of the extract molecules on Al surface. Hence, the values of $\Delta G_{\text{ads}}^\circ$ calculated were (36.1- 45.4 kJ mol^{-1}) (Table 7) again supporting the earlier proposed mixed (physisorption and chemisorption) mechanism. $\Delta G_{\text{ads}}^\circ$ value up to (-20 kJ mol^{-1}) is consistent with physical adsorption mechanism while that more negative than (-40 kJ mol^{-1}) defines chemical adsorption mechanism [32]. K_{ads} values decrease with rise in temperature (Table 7). K_{ads} values are indicative of the strength between adsorbate and adsorbent [33], their values increase with rise in temperature. This also supports the chemical mechanism, the heterogeneous factor of metal surface ($a > 0$) positive value shows that there is a molecular interaction between the layer of inhibitor and the surface of Al. Also an endothermic adsorption process ($\Delta H_{\text{ads}}^\circ > 0$) may involve chemisorption. For physisorption adsorption $\Delta H_{\text{ads}}^\circ = 41.86 \text{ kJ mol}^{-1}$ but for chemisorption adsorption $\Delta H_{\text{ads}}^\circ = 100 \text{ kJ mol}^{-1}$ [34]. Plot of ($\Delta G_{\text{ads}}^\circ$) versus T as shown in Fig.10 according to the thermodynamic basic equation:

$$\Delta G_{\text{ads}}^\circ = \Delta H_{\text{ads}}^\circ - T \Delta S_{\text{ads}}^\circ \quad (10)$$

In our results the calculated value of $\Delta H_{\text{ads}}^\circ = 93.5 \text{ kJ mol}^{-1}$ which indicates that the adsorption of the extract on Al surface is a chemisorption process. Large negative value $\Delta S_{\text{ads}}^\circ = -436 \text{ J mol}^{-1} \text{K}^{-1}$ indicates that decreasing in disorder of corrosion process on Al surface in 1 M HCl using SBE as corrosion inhibitor (Table 7).

Scanning Electron Microscopy (SEM) technique

Figure 11a shows SEM micrographs of the polished Al sample. Figure 11 b shows the SEM micrographs of Al when exposed to 1M HCl solution at room temperature in the absence of extract. This figure shows that, the Al surface appears to be very rough in the absence of extract. This is due to formation of uniform flake-type corrosion products on Al surface. No corrosion and other separate phases are visible in the micrographs. Fig.11 c shows the micrographs of the metal surface when exposed to the acid medium in the presence of 300 ppm of the extract, at the same magnification. In this micrograph the Al surface was found to be covered with smooth protective film of compounds uniformly spread over the surface as previously reported [35]. The protective film is formed due to the adsorption of the extract molecules on Al surface.

Mechanism of corrosion inhibition

Adsorption of SBE which contains fatty acid and hydrocarbon can be explained on the basis that adsorption of the extract was mainly via hetero atoms present in different constituents of extract in addition to the availability of π - electrons in the aromatic system [36]. The phytoconstituents of SBE include fatty acid and hydrocarbons such as Tannins, Flavonoids, Saponins, Cardiac glycosides, Steroids, Phlobatannins and Terpenoids, etc. The above phytochemical constituents present in SBE having many active centers at hetero atoms which are regarded as centers of adsorption. Where the results of temperatures study have shown that mechanical adsorption takes place through the chemical adsorption. It was found that Al surface in acid media has a positive charge which has vacant d- orbital [37] which leads to coordination bond of the negatively charged species. In aqueous acidic solutions, main constituents of SBE exist as neutral molecules or as protonated molecules (cations). So in view of the above the adsorption mechanism may occur as follows: First Cl^- anions adsorb chemically on positively charged Al surface, resulting that the Al surface became negatively charged. The protonated extract molecules then get adsorbed on the negatively charged Al surface.

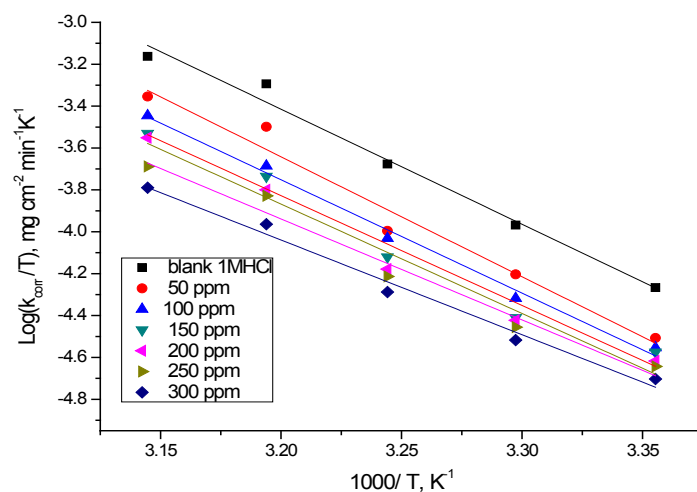


Fig. 8. Transition-state ($\log k/T$ vs. $1/T$) curves for Al in 1 M HCl with and without presence of various concentrations of SBE.

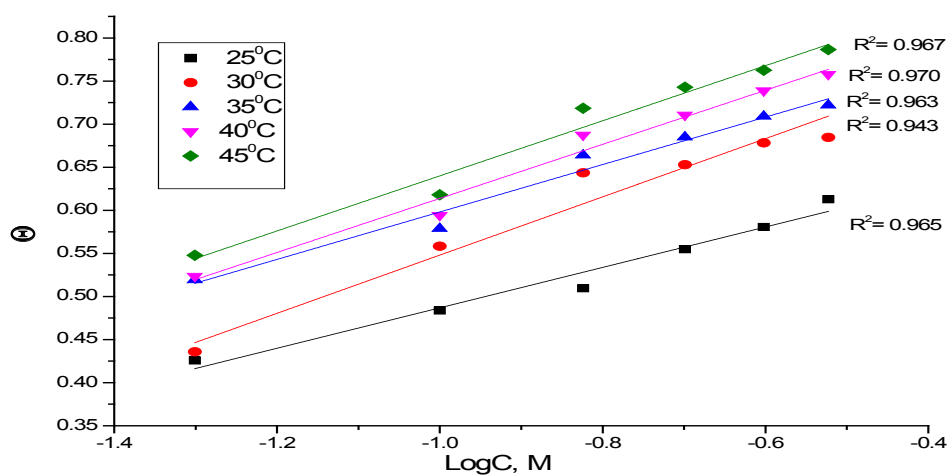


Fig. 9. Temkin adsorption plots for Al in 1 M HCl containing various doses of SBE at 25°C

TABLE 7. Thermodynamic parameters for the adsorption of SBE on Al surface in 1M HCl at various temperatures.

Temperature, K	a	Log K_{ads} M^{-1}	$-\Delta G_{ads}^{\circ}$ $kJ mol^{-1}$	ΔH_{ads}° $kJ mol^{-1}$	$-\Delta S_{ads}^{\circ}$ $J mol^{-1}K^{-1}$
298	9.8	4.571	36.1		
303	8.7	5.007	39.2		
308	8.3	5.119	40.5	93.5	436
313	8.1	5.279	42.4		
318	8.1	5.711	45.4		

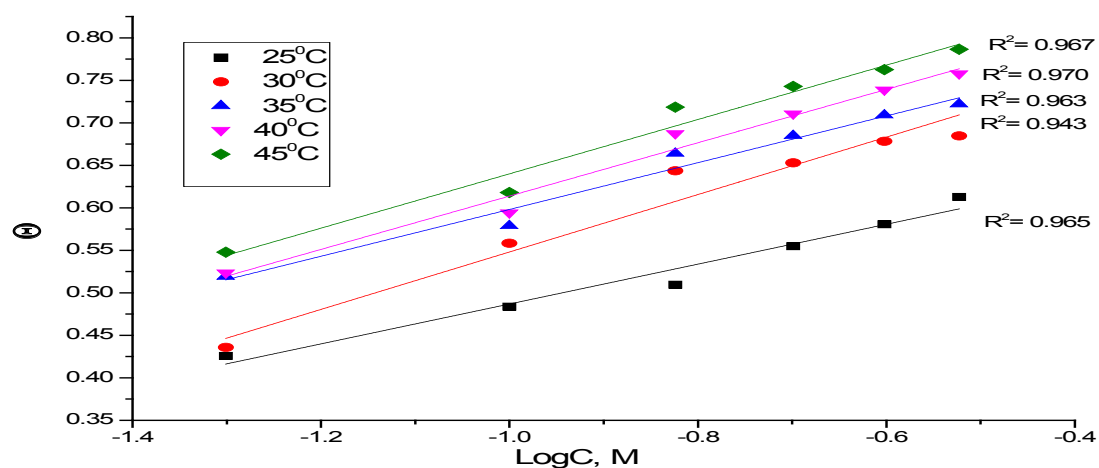


Fig. 9. Temkin adsorption plots for Al in 1 M HCl containing various doses of SBE at 25°C

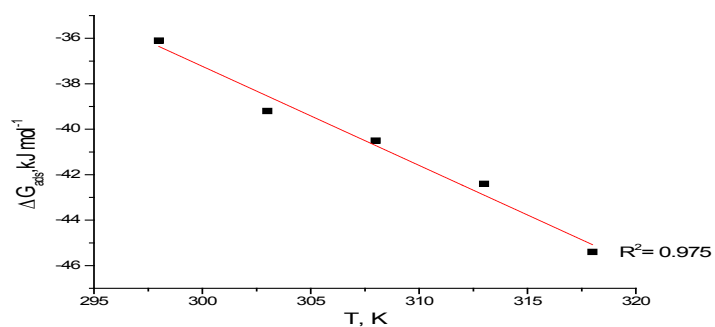


Fig.10. Variation of ΔG_{ads}° versus T for the adsorption of SBE on Al surface in 1 M HCl at different temperatures

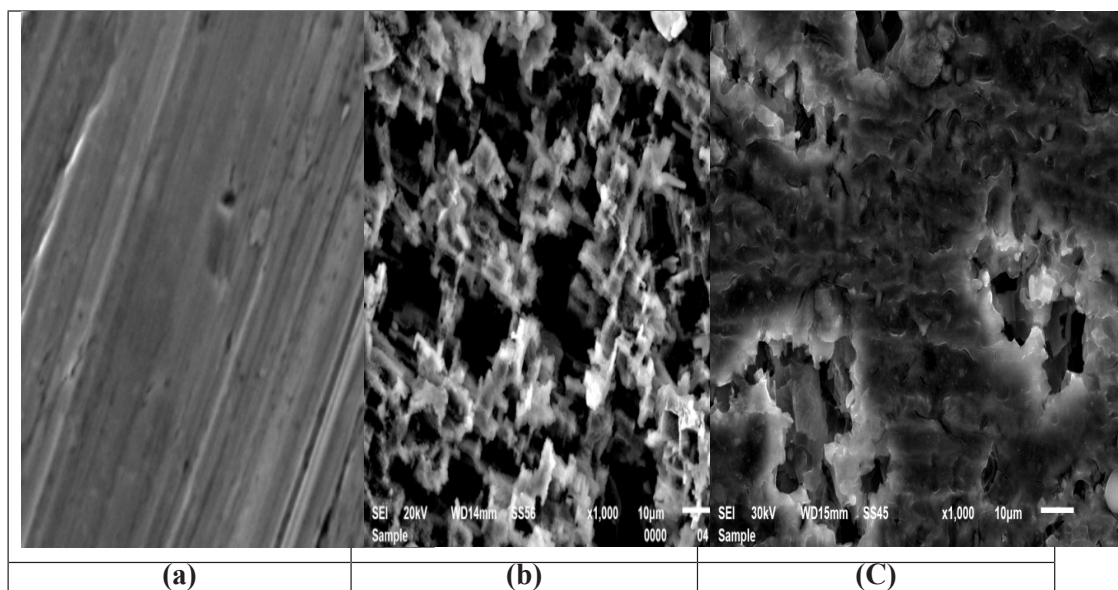


Fig. 11. SEM micrographs of Al surface (a) before immersion in 1 M HCl, (b) after 24 hr immersion in 1 M HCl and (c) after 24 hr immersion in 1 M HCl + 300 ppm of SBE at 25°C.

Conclusions

The results obtained from all methods showed that the inhibiting action increases with increases the SBE doses and with the increasing the solution temperature (chemical adsorption). Increasing the dose of the SBE, decreasing the double layer capacitances and increasing the charge transfer resistance. The adsorption of plant extract molecules on the Al surface follows Temkin adsorption isotherm. Tafel polarization results indicate that, this extract component act as mixed-type inhibitor. The inhibition efficiencies determined by WL, PP, EFM and EIS techniques are in reasonably good agreement. SEM micrographs indicate that this extract is adsorbed on Al surface forming a protective film.

References

1. Mountarlier, V., Gigandet, M.P., Normand, B., and Pagetti, J., EIS characterization of anodic films formed on 2024 aluminum alloy in sulphuric acid containing molybdate or permanganate species. *Corros. Sci.*, **47**, 937 (2005).
2. Fox PG and Bradley PA, 1,2,4-triazole as a corrosion inhibitor for copper, *Corros. Sci.*, **20**, 643 (1990).
3. El Sayed, A., Phenothiazine as inhibitor of the corrosion of cadmium in acidic solutions, *J. Appl. Electrochem.*, **27**, 193 (1992).
4. Schmitt, G., Application of Inhibitors for Acid Media: Report prepared for the European Federation of Corrosion Working Party on Inhibitors, *Br. Corros. J.*, **19**, 165 (1984).
5. Sykes, M., Silver Jubilee reviews 25 years of progress in electrochemical methods, *Br. Corros. J.* **25**, 175 (1990).
6. Chatterjee, P., Banerjee, MK. and Mukherjee, P., Synergistic inhibition of inorganic anions with pyridine-derivatives for steel in hydrochloric-acid, *Ind. J. Technol.*, **29**, 191 (1991).
7. Osman, M.M., Khamis, E. and Michael A., Corrosion inhibition of steel by triazolines in saline water, *Corros. Prev. Control*, **41**, 60 (1994).
8. Bilgic, S. and Caliskan N., An investigation of some schiff bases as corrosion inhibitors for austenite chromium nickel steel in H₂SO₄, *Appl. Electrochem.* **31**, 79 (2001).
9. Quraishi, MA. and Sardar, R., Dithiazolidines – A new class of heterocyclic inhibitors for prevention of mild steel corrosion in hydrochloric acid solution. *Corros. Sci.*, **58**, 103 (2002).
10. Okon Eddy N., I. Ita B., N. Dodo S. and D. Paul E., Inhibitive and adsorption properties of ethanol extract of Hibiscus sabdariffa calyx for the corrosion of mild steel in 0.1 M HCl., **5**, 43 (2012)
11. Eddy, N.O., Ibok, U.J. and Ebenso, E.E. J., Adsorption, synergistic inhibitive effect and quantum chemical studies of ampicillin (AMP) and halides for the corrosion of mild steel in H₂SO₄, *Appl. Electrochem.*, **40**, 445 (2010).
12. Santhanakrishnan, D., Shankar, Sripriya N. and Chandrasekaran, B., studies on the phytochemistry, spectroscopic characterization and antibacterial efficacy of salicornia brachiata, *Int J Pharm Pharmsci*, **6**, 430 (2014).
13. Mccafferty, E., Lewis Acid/Lewis Base effects in corrosion and polymer adhesion at Al surfaces, *J. Electrochem. Soc.*, **150**, 342 (2003).
14. El-Dahan, H.A., Soror T.Y. and El-Sherif R.M., Studies on the inhibition of aluminum dissolution by hexamine-halide blends, *Mater. Chem. Phys.*, **89**, 268 (2005).
15. Tao, Z., Zhang, S., Li, W. and Hou, B., Corrosion inhibition of mild steel in acidic solution by some oxo-triazole derivatives, *Corros. Sci.*, **51**, 2588 (2009).
16. Ferreira, E.S., Giacomelli, C., Giacomelli, F.C. and Spinelli, A., Evaluation of the inhibitor effect of l ascorbic acid on the corrosion of mild steel, *Mater. Chem. Phys.*, **83**, 129 (2004).
17. Paskossy, T., Impedance of rough capacitive electrodes, *J. Electroanal. Chem*, **364**, 111 (1994).
18. Growcock, F.B. and Jasinski, J.H., Time-resolved impedance spectroscopy of mild steel in concentrated hydrochloric acid = Spectroscopie d'impédance de l'acier doux dans l'acide chlorhydrique concentré, *J. Electrochem. Soc.*, **136**, 2310 (2010).
19. Abd El-Rehim, S.S., Khaled, K.F. and Abd El-Shafi, N.S., Electrochemical frequency modulation as a new technique for monitoring corrosion inhibition of iron in acid media by new thiourea derivative, *Electrochim. Acta*, **51**, 3269 (2006).
20. Lebrini, M., Lagrenee, M., Vezin, H., Gengembre L. and Bentiss, F., Electrochemical and quantum chemical studies of new thiazazole derivatives adsorption on mild steel in normal hydrochloric acid medium, *Corros. Sci.*, **47**, 485 (2005).
21. Bessone, J., Mayer, C., Tuttner, K. and Lorenz, W., AC-impedance measurements on aluminium barrier type oxide films, *J. Electrochim. Acta*, **28**, 171 (1983).

22. Kus, E. and Mansfeld, F., An evaluation of the electrochemical frequency modulation (EFM) technique, *Corros. Sci.*, **48**, 965 (2006).
23. Abdel-Rehim, S.S., Khaled, K.F. and Abd-Elshafi, N.S., Electrochemical frequency modulation as a new technique for monitoring corrosion inhibition of iron in acid media by new thiourea derivative, *Electrochim. Acta*, **51**, 3269 (2006).
24. Bockris, JO. and Swinkels, DAJ., Adsorption of decylamine on Solid Metal Electrodes, *J. Electrochem. Soc.*, **111**, 736 (1964).
25. Lee, HP. and Nobe, K., Kinetics and Mechanisms of Cu Electrodeposition in Chloride Media, *J. Electrochem. Soc.*, **133**, 2035 (1986).
26. Ashassi-Sorkhabi, H., Shabani, B., Aligholipour, B. and Seifzadeh, D., The effect of some Schiff base on the corrosion of Al in HCl solution, *Appl. Surf. Sci.*, **252**, 4039 (2006).
27. Li, Y., Zhao, P., Liang, Q. and Hou, B., Berberine as a natural source inhibitor for mild steel in 1 M H₂SO₄, *Appl. Surf. Sci.*, **252**, 1245 (2005).
28. Saleh, MM and Atia, AA, Effects of structure of the ionic head of cationic surfactant on its inhibition of acid corrosion of mild steel, *J. Appl. Electrochem.* **36**, 899 (2006).
29. Li, XH., Deng, SD. and Fu, H., Synergism between red tetrazolium and uracil on the corrosion of cold rolled steel in H₂SO₄ solution, *Corros. Sci.*, **51**, 1344 (2009).
30. Shetty, S. Divakara and Prakash S., Inhibition of mild steel corrosion in acid media by N-benzyl-N'-phenyl thiourea, *Metallic Corrosion Inhibitors*, Oxford: Pergamon Press, **27**, 216 (2008).
31. Frumkin, AN., *Zeitschrift für Physikalische Chemie*, 1925, 116, 466. [publishing corporation, New York, 1963].
32. Bhajiwala, HM. and Vashi, RT., Ethanolamine, diethanolamine and triethanolamine as corrosion inhibitors for zinc in binary acid mixture (HNO₃ + H₃PO₄), *Bull. Electrochem.*, **17**, 441 (2001).
33. Umoren, SA., Inhibition of aluminum and mild steel corrosion in acidic medium using Gum Arabic, *Cellulose*, **15**, 751 (2008).
34. Oguzie, EE., Li, Y. and Wang, FH., Corrosion effect of allylthiourea on bulk nanocrystalline Ingot iron in diluted acidic sulphates solutions, *Electrochim. Acta*, **52**, 3950 (2007).
35. Mehaute, AH. and Grepy, G., Introduction to transfer and motion in fractal media: The geometry of kinetics, *Solid State Ionics*, **9-10**, 17 (1989).
36. Khaled, KF., Molecular simulation, quantum chemical calculations and electrochemical studies for inhibition of mild steel by triazoles, *Electrochim. Acta*, **53**, 3484 (2008).
37. Desai, MN., Corrosion inhibitors for aluminum alloys: A review, *Werkst. Korros.*, **23**, 475 (1972).

(Received : 27/2/ 2017;
accepted : 2 /4 / 2017)

تآكل الألومنيوم في محلول حمض الهيدروكلوريك

عبدالعزیز السيد فودة^١، صلاح الدين محمود رشوان^٢، عائشة أمام محمد^٣، عائشة محمود إبراهيم^٤
قسم الكيمياء – كلية العلوم – جامعة المنصورة وقسم الكيمياء – كلية العلوم – جامعة قناة السويس
الأسماعيلية - مصر.

يعطينا هذا البحث نبذة عن أهمية الألومنيوم حيث أنه يدخل في العديد من التطبيقات الصناعية لأنه يمتلك كثافة قليلة ووزن خفيف وتوصيلية حرارية عالية وبالرغم من ذلك فهو عنصر نشط ويتعرض للتآكل وهذا البحث يدرس كيفية حماية الألومنيوم من التآكل.

تم دراسة تأثير مستخلص نبات الساليكورنيا كمثبط لتآكل الألومنيوم في محلول من حمض الهيدروكلوريك تركيزه ١ مولر باستخدام طريقة الفقد في الوزن (WL) وطريقة المعاوقة الكهربية (EIS) والتردد الكيميائي المعدل (EFM) والاستقطاب البوتنشيو ديناميكي (pp) وقد تم التوصل الي ان مستخلص نبات الساليكورنيا يعمل كمثبط طبيعي جيد لتآكل الألومنيوم في المحلول الحمضي.

ووجدنا أن كفاءة التثبيط ازدادت بزيادة تركيز المستخلص وأيضا بزيادة درجة الحرارة وهذا يوضح أن التثبيط يحدث نتيجة إمتزاز المستخلص كيميائيا علي سطح الالومنيوم.

أثبتت دراسة طريقة الاستقطاب البوتنشيو ديناميكي أن هذا المستخلص يعمل كمثبط مزدوج التأثير وقد توصلت دراسة طريقة المعاوقة الكهربية الي انه يوجد اختزال في كثافة الطبقة المزدوجة وزيادة في المقاومة لانتقال الشحنات الكهربية.

ووجدنا أن امتصاص هذا المستخلص علي سطح الالومنيوم يتبع طريقة (Temkin) وقد وجد أن هذا المستخلص يكون طبقة جيدة تحمي سطح الألومنيوم من التآكل في محلول حمض الهيدروكلوريك وأيضا تم دراسة سطح الالومنيوم باستخدام طريقة (SEM).

تم التوصل الي أن كل النتائج التي حصلنا عليها من كل الطرق المستخدمة السابقة متوافقة مع بعضها بدرجة كبيرة.